Non-Rayleigh signal of interacting quantum particles

M. F. V. Oliveira,[1] F. A. B. F. de Moura,[1] A. M. C. Souza,[2] M. L. Lyra,[1] and G. M. A. Almeida[1,*]
[1]*Instituto de Física, Universidade Federal de Alagoas, 57072-900 Maceió, Alagoas, Brazil*
[2]*Departamento de Física, Universidade Federal de Sergipe, 49100-000 São Cristóvão, Sergipe, Brazil*

(Received 3 May 2023; accepted 16 August 2023; published 24 August 2023)

The dynamics of two interacting quantum particles on a weakly disordered chain is investigated. Spatial quantum interference between them is characterized through the statistics of two-particle transition amplitudes, related to Hanbury Brown-Twiss correlations in optics. The fluctuation profile of the signal can discern whether the interacting parties are behaving like identical bosons, fermions, or distinguishable particles. An analog fully developed speckle regime displaying Rayleigh statistics is achieved for interacting bosons. Deviations toward long-tailed distributions echo quantum correlations akin to noninteracting identical particles. In the limit of strong interaction, two-particle bound states obey compound Rician distributions.

DOI: 10.1103/PhysRevA.108.023520

I. INTRODUCTION

Anderson localization is a universal phenomenon that underlies wave physics [1]. It results from the destructive interference of the waves due to a random potential. In quantum mechanics, the problem is often addressed for noninteracting particles. However, interaction can lead to involved physics such as many-body localization, which has recently seen significant progress [2]. The exponential growth of dimensionality in an interacting multiparticle system makes it very challenging to explore those effects.

Yet a system involving only two interacting particles delivers a rich set of features [3–11]. Earlier studies addressed the conditions in which the interaction lead to an increase of the localization length compared to the noninteracting case. It started with the observation that in a disordered chain two interacting electrons could propagate on a distance much larger than one-particle localization length would allow for [12]. In the numerous works that followed, such an enhancement mechanism in the presence of moderate particle-particle interaction and its scaling properties was explored in more depth [13–17]. The enhancement of the localization length was also reported in quasiperiodic chains [18] and explained in terms of a resonant mixing of the noninteracting two-particle eigenstates [19].

Classical and quantum correlations have been explored in two-particle systems even in the absence of interaction [4,5]. The quantum correlations in this case originate from the symmetrization of the wave functions to accommodate the bosonic or fermionic character of the particles [7]. Furthermore, two-particle systems enjoy a convenient photonic implementation based on a square waveguide lattice using only classical sources of light [6,7,9,11,20].

The interplay between interaction and disorder in those systems is not trivial [17] and depends on a number of factors, including the property that is being measured. Most characterizations require knowledge of many wave-function amplitudes at a time (e.g., the participation ratio [11,19]). In this work we propose another route to obtain relevant information about the system. We are interested in the statistics of successive measurements of Hanbury Brown-Twiss type of correlations from a *local* standpoint. In a coupled waveguide array [9] that means monitoring the beam intensity in a single waveguide. It accounts for the joint probability of finding the particles at specific locations. The procedure above yields speckle patterns to which we obtain all the associated distributions in detail. Surprisingly, the speckle contrast is able to precise the particle identity and the degree of interaction between them. It shows up as specific deviations from the exponential fully developed speckle regime.

Tailored speckle generation finds a handful of applications [21]. Our main goal here, though, is to explore the following question: what can a local speckle statistics tell us about the nature of the physical mechanisms involved in its generation? As an example, the authors of Ref. [22] explored the statistics of two-photon speckles as a mean to disclose relevant information about their entanglement properties. The statement above is particularly appealing to rogue wave phenomena in optical and quantum systems. There has been a renewed interest in the role of disorder on the generation of rare and short-lived wave amplitude spikes [23,24]. In a recent work, Kirkby *et al.* [25] addressed Fock-space caustics in simple Bose-Hubbard models, which are also related to rogue events. Here we realize that intrinsic quantum correlations due to particle identity lead to long-tailed distributions. Rogue waves are often studied as emergent phenomena in nonlinear Schrödinger equations [26] that describe, for instance, Bose-Einstein condensates [27]. A bottom-up approach should therefore unveil the key linear elements responsible for driving anomalous fluctuations in quantum systems.

II. HAMILTONIAN MODEL

Let us start by considering two interacting distinguishable particles (e.g., two electrons with opposite spins) in a linear

*gmaalmeida@fis.ufal.br

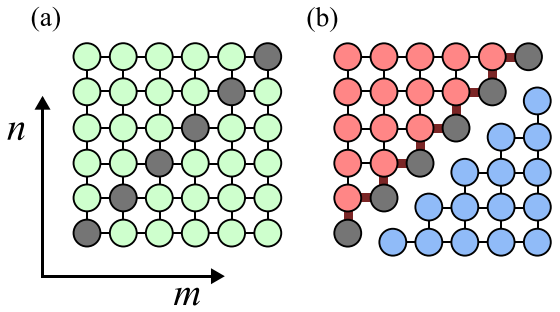

FIG. 1. Two-particle Hamiltonian graph structure. (a) The state space of two distinguishable particles in one dimension can be mapped onto a 2D array. Diagonal vertices represent states with double occupation (bound states). (b) By exploiting the symmetry with respect to the diagonal, the basis change $|mn\rangle^{\pm} = (|mn\rangle \pm |nm\rangle)/\sqrt{2}$ decouples the Hamiltonian into one describing identical bosons (upper red vertices) and another accounting for spinless fermions (lower blue vertices). In the bosonic case, the coupling between bound states with the other vertices are renormalized by $\sqrt{2}$ (thick edges). Considering a 2D photonic waveguide implementation, each of these subspaces is achieved by setting the proper relative phase between two input beams at positions (m, n) and (n, m). Note that such a decoupling is valid despite the strengths of disorder W and interaction U.

chain with N sites described by the Hamiltonian ($\hbar = 1$)

$$H = J\sum_{j=1}^{N-1}(a_{j+1}^{\dagger}a_j + b_{j+1}^{\dagger}b_j + \text{H.c.}) + \sum_{j=1}^{N}[\epsilon_j(a_j^{\dagger}a_j + b_j^{\dagger}b_j) + U a_j^{\dagger}a_j b_j^{\dagger}b_j], \quad (1)$$

where a_j, b_j ($a_j^{\dagger}$, $b_j^{\dagger}$) are the corresponding annihilation and creator operators at site j. U is the local particle (respulsive) interaction strength, J is the nearest-neighbor hopping constant, and ϵ_j is the onsite potential which we set randomly within the uniform interval $[-W/2, W/2]$, with W being the disorder width. The Hilbert space is spanned by N^2 two-particle states $|mn\rangle = b_n^{\dagger}a_m^{\dagger}|0\rangle$, where $|0\rangle$ is the vacuum state.

It is known that a basis change of the form $|mn\rangle^{\pm} = (|mn\rangle \pm |nm\rangle)/\sqrt{2}$ ($m \neq n$), with respect to the "diagonal" double occupancy (bound) states, decouple the Hamiltonian in two parts [7]. The symmetric combinations alongside bound states interact via a Bose-Hubbard Hamiltonian. The antisymmetric part behave as noninteracting spinless fermions. Figure 1 depicts their state-space structure. Any speckle pattern of the intensities will therefore be controlled by those bosonic and fermionic subspaces, each playing a distinct role.

III. QUANTUM UNITARY DYNAMICS AND ITS SPECKLE ANALOG

Before we elaborate on the speckle formalism for the two-particle dynamics, it is appropriate to address the wavefunction statistics on a single-particle tight-binding model $H^{(1)} = J\sum_j(a_{j+1}^{\dagger}a_j + \text{H.c.}) + \sum_j \epsilon_j a_j^{\dagger}a_j$. Consider the transition amplitude between sites m and p due to the time evolution operator $\mathcal{U} = e^{-iH^{(1)}t}$,

$$f_m^p = \langle p|\mathcal{U}|m\rangle = \sum_k a_k e^{-iE_k t} = Ae^{i\theta}, \quad (2)$$

where $A = A(m, p; t)$, $\theta = \theta(m, p; t)$, and the lengths $a_k = a_k(m, p) = v_{k,m}v_{k,p}$ read from the eigenfunctions $v_{k,j} = \langle j|E_k\rangle$ of $H^{(1)}$.

Despite describing a deterministic time evolution, the phasor sum above can effectively be treated as a random one. Note that $\text{Re}\{f_m^p\} = \sum_k a_k \cos(E_k t)$ and $\text{Im}\{f_m^p\} = -\sum_k a_k \sin(E_k t)$. As the state evolves in time, the phase $E_k t$ covers the interval $[0, 2\pi)$ uniformly. If the evolution is truncated in time steps $\Delta t \gg J^{-1}$, the resulting amplitude statistics in the *time domain* is equivalent to that obtained by sorting those phases at random, with fixed individual phasor lengths a_k. In other words, each time step works as one realization of a series of random phases.

When the disorder is weak (meaning a large localization length) it is reasonable to assume $a_k \sim 1/N$. If we let the state evolve long enough, the central limit theorem applies and thus the real and imaginary parts of f_m^p asymptotically reach circular Gaussian statistics (with standard deviation σ) centered at zero. In turn, A obeys the Rayleigh distribution $p_A(A) = (A/\sigma^2)\exp(-A^2/2\sigma^2)$, where σ is the scale parameter. The corresponding argument θ is uniformly distributed in the full cycle [28]. The intensity $I = A^2$ then follows the exponential distribution $p_I(I) = p_A(\sqrt{I})|dA/dI| = s^{-1}e^{-I/s} \equiv \text{Exp}(s)$, with mean intensity $\langle I\rangle = s = 2\sigma^2$. Note that no average over disorder realizations is being considered here. The above statistical framework is valid for a single disorder realization and built on the truncated time evolution of the wave function [29].

We can also make use of the central limit theorem in the case of a pure chain ($\epsilon_j = \epsilon$), with $v_{k,j}$ being Bloch functions. Now, the particle-hole symmetry entails $E_k = -E_{-k}$ and $a_k = \pm a_{-k}$ depending on the chosen pair of locations m and p. Either way, we end up with $A = |\text{Re}\{f_m^p\}|$ or $A = |\text{Im}\{f_m^p\}|$. In such a particular case, A follows a half-normal distribution and thus $x = I/\sigma^2$ has a chi-squared distribution with one degree of freedom, $p_I(x) = e^{-x/2}/\sqrt{2\pi x}$.

As we will see in what follows, a variety of speckles are obtained depending on the nature of the particles, their interaction, and initial configuration. A relevant measure to discriminate between them is the ratio between the standard deviation of the intensity σ_I by its mean, namely, the contrast $C = \sigma_I/\langle I\rangle$. A fully developed speckle obeying exponential statistics renders $C = 1$. This gives us a reference value to evaluate the degree of fluctuations of a given speckle pattern.

IV. TWO-PARTICLE SPECKLES

A. Noninteracting particles

Now that we visualize the single-particle quantum evolution as a random process over time, let us extended it to the case of two distinguishable particles when $U = 0$. Considering an input prepared at sites (m, n), the transition to (p, q), $h_{mn}^{pq} = \langle pq|e^{-iHt}|mn\rangle$, reads

$$h_{mn}^{pq} = f_m^p f_n^q = A_1 A_2 e^{i(\theta_1+\theta_2)}. \quad (3)$$

The corresponding intensity is analogous to the two-particle correlation function $\langle a_m^\dagger b_n^\dagger b_n a_m\rangle$, known as Hanbury Brown-Twiss correlations in optics [4,5,8,11]. Each individual intensity in Eq. (3) follows an exponential distribution $I_i = A_i^2 \sim \mathrm{Exp}(s_i)$. If we let I_1 and I_2 be independent random variables, it can be shown that their product $I = I_1 I_2$ obeys the K distribution [30]

$$\mathcal{K}(I;\mu,\nu) = \frac{2\nu}{\mu\Gamma(\nu)}\left(\sqrt{\frac{I}{\mu}\nu}\right)^{\nu-1} K_{\nu-1}\left(2\sqrt{\frac{I}{\mu}\nu}\right), \qquad (4)$$

with shape parameter $\nu = 1$. Therein $K_\nu(x)$ is a modified Bessel function of the second kind of order ν and $\mu = s_1 s_2$ is the mean intensity. The speckle contrast for the K distribution reads $C(\nu) = \sqrt{(\nu+2)/\nu}$. Hence, larger fluctuations are expected when two distinguishable particles are involved, that is, $C = \sqrt{3} \approx 1.73$, even in the absence of interaction. We highlight that K distributions arise whenever some speckle intensity is known to obey exponential statistics but there is uncertainty about its mean [28,31].

Previously we assumed that I_1 and I_2 were independent. This is true for most input (m,n) and output (p,q) location pairs. However, some residual correlations can be present. This happens, for instance, when $|p-m| = |q-n|$ and disorder is weak. Both intensities become fully correlated ($I_1 = I_2$) when the transition amplitude involve only bound states, i.e., $|h_{mm}^{pp}| = |f_m^p|^2 \sim \mathrm{Exp}(s)$. The intensity $I = |f_m^p|^4$ then obeys a Weibull distribution $p_I(y) = \alpha^{-1}(2y)^{-1/2}e^{-\sqrt{2y}}$, where $y = I/\alpha$ and $\alpha = 2s^2$ is the mean intensity. The contrast now reads $C = \sqrt{5} \approx 2.24$.

The long-tailed character of the speckles generated by noninteracting distinguishable particles stems from the spectral correlations of the two-particle Hamiltonian [Eq. (1)]. When $U = 0$ its diagonal form reads $H = \sum_{k_1,k_2}^N E_{k_1k_2} b_{k_2}^\dagger a_{k_1}^\dagger |0\rangle\langle 0| a_{k_1} b_{k_2}$, with $|0\rangle$ being the vacuum and $E_{k_1k_2} = E_{k_1} + E_{k_2}$. As such the N^2 phases $E_{k_1k_2}t$ are combinations of two identical sets of N single-particle inputs. Based on the two-dimensional (2D) mapping (Fig. 1), the observed speckles featuring higher contrasts are the result of structural correlations. Shortly, we will see that those correlations are partially destroyed when $U \neq 0$.

Let us now discuss the speckle profile of identical bosons and spinless fermions separately. In a photonic waveguide array, each set can be explored by injecting two coherent beams at locations (m,n) and (n,m) with the proper symmetric or antisymmetric phase relationship [7,11]. Given an input $|\psi(0)\rangle = (b_n^\dagger a_m^\dagger \pm b_m^\dagger a_n^\dagger)|0\rangle$ the transition amplitudes read $h_{mn(B)}^{pq} = (f_m^p f_n^q + f_m^q f_n^p)\mathcal{N}$, with $\mathcal{N} = 2^{-(\delta_{mn}+\delta_{pq})/2}$, for bosons and $h_{mn(F)}^{pq} = f_m^p f_n^q - f_m^q f_n^p$ for fermions. In both cases there is interference between K-distributed speckles. This is expected since we are now dealing with entangled input states.

Indeed, the quantum correlations manifest in the speckle statistics by delivering weaker fluctuations than those promoted by distinguishable particles. To see this, consider (bound states excluded) $f_m^p f_n^q \pm f_m^q f_n^p = A_1 e^{i\theta_1} + A_2 e^{i\theta_2}$ is a two-component random phasor sum with independent K-distributed amplitudes $A_i \sim 2\sqrt{I_i}\mathcal{K}(\sqrt{I_i};\mu,1)$ with mean $\langle A_i\rangle = \pi\sqrt{\mu}/4$ and uniformly distributed phases θ_i. Note that we are assuming a common mean for both variables. This is a reasonable assumption for a weakly disordered chain. The output intensity speckle can be evaluated by means of a version of a modified Kluyver-Pearson formula [32]. It results in another K distribution [see Eq. (4)], now with shape parameter $\nu = 2$ and mean $\mu' = 2\mu$, that is, $p_I(I) = \mathcal{K}(I;\mu',2)$. The contrast is now $C = \sqrt{2} \approx 1.41$, lower than that obtained for distinguishable particles ($C = \sqrt{3}$). Note that the entanglement due to wave-function symmetrization modifies the classical speckle signal. Figure 2(a) displays all the distributions obtained so far in agreement with the numerical simulations.

B. Interacting particles

We are now ready to see how the presence of a local interaction between both particles modifies the speckle statistics. When $U \neq 0$ transition amplitudes between the quantum states can no longer be expressed in terms of single-particle wave functions. This symmetry loss in the two-particle spectrum tends to drive the intensity statistics toward the exponential regime. However, when we expand the dynamics in terms of the bosonic and fermionic subspaces (see Fig. 1), the latter is not affected by U. A given input $b_n^\dagger a_m^\dagger|0\rangle$ will evolve independently in each one of those subspaces, having symmetric and antisymmetric components. The fermionic part maintains its K-distributed profile $\mathcal{K}(I;\mu',2)$. For now, it thus suffices to examine transitions between bosonic states against U.

Figure 3 shows the contrast C for several values of the interaction U within distinct timescales. When $U \ll J$, exponential statistics is only obtained in the long-time regime. As the hitherto noninteracting bosonic spectrum is slightly altered it takes awhile before the random phasor sum converges to a fully developed speckle [see Fig. 2(b)]. When U is weak, whether or not both bosons are loaded in the same site, the short-time regime typically features higher fluctuations. Figure 3(a) [Fig. 3(b)] indicates that these fluctuations are reminiscent of the speckle pattern associated to the K distribution (Weibull distribution). For intermediate values of U that transient dynamics becomes less pronounced and the speckle pattern rapidly becomes exponentially distributed.

As U increases further, a smaller band of N bound (B) states builds up apart from the scattering (S) part of the spectrum consisting of $N(N-1)/2$ states [3,8]. It is then convenient to express the transition amplitude as the phasor sum of the form $h_{mn(B)}^{pq} = \sum_{k\in S} b_k e^{i\phi_k} + \sum_{k'\in B} b'_k e^{i\phi'_k}$. When $U \gg J$, if both bosons are injected in different sites they will display fermion-like correlations such as spatial antibunching [8] as the phasor sum running over the bound states becomes negligible. This is heralded as the high contrast seen in Fig. 3(a) at short and intermediate timescales. Yet, although transitions between scattered and bound states always remain negligible in this case, the speckle will eventually set as a fully developed one ($C \approx 1$). That is, the antibunching dynamics lasts indefinitely for the repelling bosons, but the phase relationships embedded in the corresponding phasor sum bring the central limit theorem to hold, unless $U \to \infty$ (hard-core limit).

We now realize that when loading two distinguishable particles in different locations (m,n), the resulting speckle

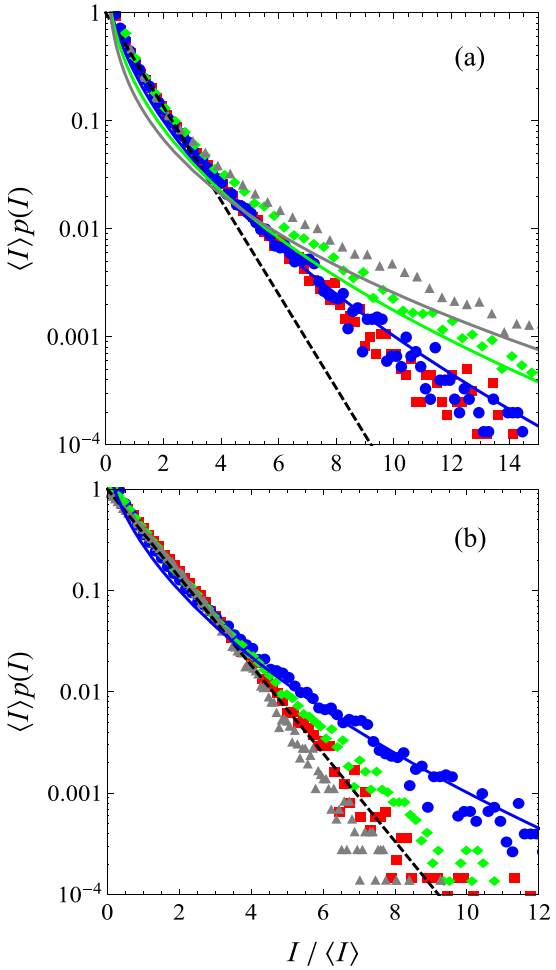

FIG. 2. Scaled probability density functions of two-particle intensities for a single sample of a disordered array featuring $N = 40$ sites and $W = 0.01J$. The statistics is taken from many operations of e^{-iHt} up to $tJ = 10^7$ in steps of size 100. (a) Noninteracting case ($U = 0$). Two particles are prepared at sites $(m, n) = (20, 22)$ and the intensity $I = |h^{pq}_{mn}|^2$ measured at $(p, q) = (23, 26)$. The output for distinguishable particles is shown as green diamonds, with the corresponding K-distribution function with shape parameter $\nu = 1$ (green curve) with contrast $C = \sqrt{3}$. When both particles are identical bosons or fermions with properly symmetrized input-output kets the intensity reads $I = |h^{pq}_{mn(B)}|^2$ and $I = |h^{pq}_{mn(F)}|^2$, respectively (red squares and blue circles). For both cases we get another K distribution with shape parameter $\nu = 2$ and (blue curve) contrast $C = \sqrt{2}$ as a consequence of entanglement due to wave-function symmetrization. Gray triangles represent a transition between bound states, $I = |h^{pp}_{mn}|^2$, with $m = 20$ and $p = 22$. In this case, only the bosonic subspace is involved. The solid gray curve represents the fitting Weibull distribution ($C = \sqrt{5}$). For reference, the exponential distribution is shown as the dashed black curve. (b) Interacting case ($U = 1J$). The same quantities are plotted. Now, all the data approach the exponential distribution but that corresponding to identical fermions (not affected by U). The bosonic distribution (red squares) fits the most whereas that corresponding to distinguishable particles displays an extended tail. When only bound states (gray triangles) are involved the tail retracts. This signalizes the onset of modes with a shorter localization length.

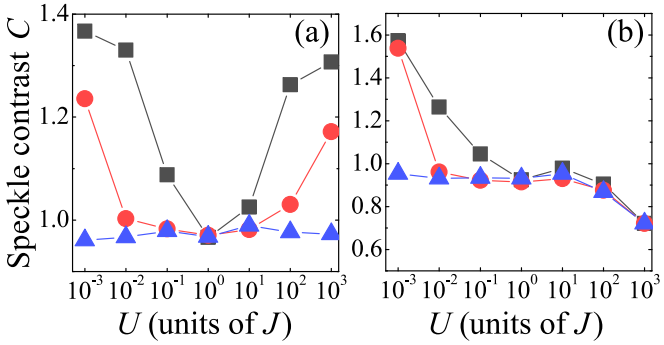

FIG. 3. Bosonic speckle contrast C against interaction strength U on a chain with $N = 26$ sites and $W = 0.01J$. For a given disorder sample, the statistics for $I = |h^{pq}_{mn(B)}|^2$ is taken within three distinct time windows, namely, short ($tJ \in [0, \Delta]$; squares), intermediate ($tJ \in [10^6, 10^6 + \Delta]$; circles), and long ($tJ \in [10^9, 10^9 + \Delta]$; triangles), with $\Delta = 10^5$, in steps of 100. Contrast curves are averaged over 100 independent realizations of disorder. In (a) two bosons are loaded at sites (10,11), with the intensity measurements being taken at (13,16). Panel (b) depicts the case of bound states, with the two bosons placed at (10,10) and measured at (11,11). Contrast $C = 1$ corresponds to a fully developed speckle (exponential intensity statistics).

in (p, q) comes as an interference between Rayleigh- and K-distributed phasors (bosonic and fermionic components, respectively). Figure 2(b) shows that the speckle is nearly exponentially distributed aside from a pronounced tail (the contrast is numerically found to be $C \approx 1.05$). Here, the fermionic correlations associated to the antisymmetric subspace forbid the formation of a fully developed speckle. Therefore, such a contrast $C > 1$ will always hold in the limit of infinite time evolution of interacting distinguishable particles for any U/J, in the regime of weak disorder $W \ll J$. If the disorder were higher, the speckle contrast would be lower due to the onset of strongly localized Anderson modes. In the following we discuss a related scenario that involves bound states in the large U/J regime.

C. Bound states and sub-Rayleigh statistics

A noteworthy trend that occurs in the regime of strong interaction U is the decrease in contrast when both input and output involves bound states [see Fig. 3(b)]. A tail retraction can already be noticed for intermediate U [compare the triangles with the reference exponential curve in Fig. 2(b)]. This can be readily explained in terms of the energy pulling effect taking place in the band of bound states [3,8]. Even if the disorder $W \ll J$, the effective hopping strength within the band will eventually diminish to the point that strongly localized bound states prevail. It fosters asymmetry between the amplitudes in a random phasor sum. One or a few phasors will stand out compared to the remaining terms that amount to an exponentially distributed intensity with mean s_n.

In the simplest case of a single dominant phasor with intensity I_0, we get the Rician distribution [28]

$$R(I; r) = s_n^{-1} e^{-(r+I/s_n)} \mathcal{I}_0(2\sqrt{Ir/s_n}), \tag{5}$$

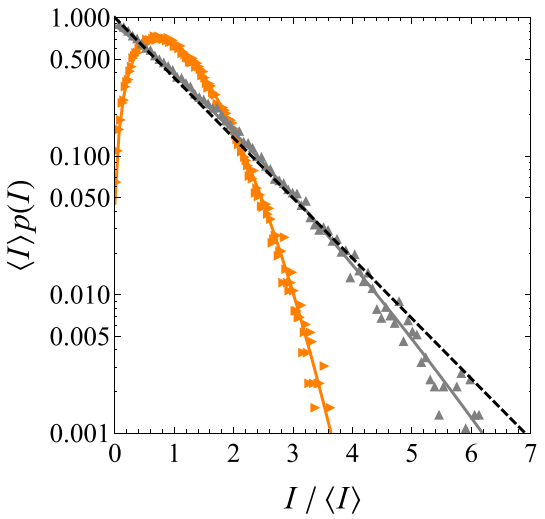

FIG. 4. Scaled probability density functions associated to bosonic bound-state transitions. Here, $I = |h^{pp}_{mm}|^2$, with $m = 20$ and $p = 22$, considering a chain with $N = 40$ sites in the strong U regime. Statistics is taken on a single disorder sample with $W = 0.01J$ evolving up to time $tJ = 10^7$ in steps of 100. Up (right) Triangles represent the case for $U = 200J$ ($U = 500J$). Solid curves are the compound Rician fittings obtained by isolating the four greatest amplitudes of the corresponding random phasor sum to build $g(r)$ (see text). The exponential distribution is displayed as the dashed curve for reference.

where $\mathcal{I}_0(x)$ is the modified Bessel function of the first kind of order zero and $r = I_0/s_n$. The contrast in this case is $C(r) = \sqrt{1+2r}/(1+r)$. If more than one dominant phasors is set apart we can compound the distribution above over different r to obtain $p_I(I) = \int R(I|r)g(r)dr$ where $R(I|r)$ is the Rician distribution conditioned on knowledge of r and $g(r)$ is its probability density function.

The above generalized form of Rician distributions will also display a lower contrast compared with a fully developed speckle. It ultimately depends on U as well as the distance between input and output sites given the typical spatial profile of localized modes. (It is important to mention that there is a nonmonotonic relationship between U and the degree of Anderson localization in disordered two-particle systems [19].) That is, if such a distance is large enough we expect $g(r) \sim \mathrm{Exp}(s_0)$ and then the Rician compound turns into an exponential distribution with mean $\langle I\rangle = s_n + s_0$.

To see the compound Rician distributions in operation, let us turn our attention to the regime of strong U. Figure 4 confirms the predicted statistics for short-haul transitions involving bound states. The integral $\int R(I|r)g(r)dr$ is evaluated numerically. The necessary number of phasors involved to make $g(r)$ depends on both U and the distance between input and output locations. When the distribution is nearly exponential, the standard Rician distribution with only one dominant phasor ($g(r)$ being a Dirac delta function) should be enough. Sub-Rayleigh statistics can thus be obtained for strongly interacting particles in a weak disordered media.

V. CONCLUSION

In summary, we have seen that fluctuations associated to local intensity measurements can disclose subtle quantum correlations. Non-Rayleigh speckles can be extracted from the time evolution of two quantum particles. They range from low contrast forms obeying compound Rician distributions to K-distributed speckles that display higher-than-exponential fluctuations. The two-particle dynamics can be promptly adapted to a square photonic waveguide array loaded with classical light [6,7,9,11,20]. The different speckle patterns is then obtained upon setting the desired input phase relationship (so as to activate bosonic and/or fermionic behavior) and controlling the detuning between the diagonal waveguides and the others [20].

Besides having immediate applications is optics, our results apply to the characterization of quantum systems in general. We showed that local measurements in the computational basis is able to capture subtle quantum correlations involving identical particles. Even when both particles are distinguishable their resulting speckle distribution display a contrast $C > 1$, a property that can be traced back to fermionic correlations. The speckle corresponding to two bosonic particles also feature a higher contrast in both weak and strong U limits. It takes a transient time before their intrinsic correlations are washed out and we get a fully developed speckle. This is an interesting feature that allows one to manipulate the speckle statistics while maintaining the overall dynamical pattern [21]. This is yet another manifestation of entanglement due to particle identity that meets practical applications [33].

We mention that related studies involving two-photon speckle statistics as a probe of entanglement can be found in Refs. [22,34]. Future works may delve into the speckle response at the multiparticle level [35,36] and its relationship with other forms of entanglement.

ACKNOWLEDGMENT

This work was supported by CNPq, CAPES (Brazilian agencies), and FAPEAL (Alagoas state agency).

[1] F. Evers and A. D. Mirlin, Anderson transitions, Rev. Mod. Phys. **80**, 1355 (2008).

[2] D. A. Abanin, E. Altman, I. Bloch, and M. Serbyn, Colloquium: Many-body localization, thermalization, and entanglement, Rev. Mod. Phys. **91**, 021001 (2019).

[3] K. Winkler, G. Thalhammer, F. Lang, R. Grimm, J. Hecker Denschlag, A. J. Daley, A. Kantian, H. P. Büchler, and P. Zoller, Repulsively bound atom pairs in an optical lattice, Nature (London) **441**, 853 (2006).

[4] Y. Bromberg, Y. Lahini, R. Morandotti, and Y. Silberberg, Quantum and Classical Correlations in Waveguide Lattices, Phys. Rev. Lett. **102**, 253904 (2009).

[5] Y. Lahini, Y. Bromberg, D. N. Christodoulides, and Y. Silberberg, Quantum Correlations in Two-Particle Anderson Localization, Phys. Rev. Lett. **105**, 163905 (2010).

[6] A. Peruzzo, M. Lobino, J. C. F. Matthews, N. Matsuda, A. Politi, K. Poulios, X.-Q. Zhou, Y. Lahini, N. Ismail, K. Wörhoff, Y. Bromberg, Y. Silberberg, M. G. Thompson, and J. L. OBrien,

Quantum walks of correlated photons, Science **329**, 1500 (2010).

[7] D. O. Krimer and R. Khomeriki, Realization of discrete quantum billiards in a two-dimensional optical lattice, Phys. Rev. A **84**, 041807(R) (2011).

[8] Y. Lahini, M. Verbin, S. D. Huber, Y. Bromberg, R. Pugatch, and Y. Silberberg, Quantum walk of two interacting bosons, Phys. Rev. A **86**, 011603(R) (2012).

[9] G. Corrielli, A. Crespi, G. Della Valle, S. Longhi, and R. Osellame, Fractional bloch oscillations in photonic lattices, Nat. Commun. **4**, 1555 (2013).

[10] G. Dufour and G. Orso, Anderson Localization of Pairs in Bichromatic Optical Lattices, Phys. Rev. Lett. **109**, 155306 (2012).

[11] C. Lee, A. Rai, C. Noh, and D. G. Angelakis, Probing the effect of interaction in anderson localization using linear photonic lattices, Phys. Rev. A **89**, 023823 (2014).

[12] D. L. Shepelyansky, Coherent Propagation of Two Interacting Particles in a Random Potential, Phys. Rev. Lett. **73**, 2607 (1994).

[13] Y. Imry, Coherent propagation of two interacting particles in a random potential, Europhys. Lett. **30**, 405 (1995).

[14] Y. V. Fyodorov and A. D. Mirlin, Statistical properties of random banded matrices with strongly fluctuating diagonal elements, Phys. Rev. B **52**, R11580 (1995).

[15] F. von Oppen, T. Wettig, and J. Müller, Interaction-Induced Delocalization of Two Particles in a Random Potential: Scaling Properties, Phys. Rev. Lett. **76**, 491 (1996).

[16] I. V. Ponomarev and P. G. Silvestrov, Coherent propagation of interacting particles in a random potential: The mechanism of enhancement, Phys. Rev. B **56**, 3742 (1997).

[17] R. A. Römer and M. Schreiber, No Enhancement of the Localization Length for Two Interacting Particles in a Random Potential, Phys. Rev. Lett. **78**, 515 (1997).

[18] S. Flach, M. Ivanchenko, and R. Khomeriki, Correlated metallic two-particle bound states in quasiperiodic chains, Europhys. Lett. **98**, 66002 (2012).

[19] W. S. Dias, E. M. Nascimento, M. L. Lyra, and F. A. B. F. de Moura, Dynamics of two interacting electrons in anderson-hubbard chains with long-range correlated disorder: Effect of a static electric field, Phys. Rev. B **81**, 045116 (2010).

[20] S. Longhi and G. D. Valle, Tunneling control of strongly correlated particles on a lattice: A photonic realization, Opt. Lett. **36**, 4743 (2011).

[21] Y. Bromberg and H. Cao, Generating Non-Rayleigh Speckles with Tailored Intensity Statistics, Phys. Rev. Lett. **112**, 213904 (2014).

[22] C. W. J. Beenakker, J. W. F. Venderbos, and M. P. van Exter, Two-Photon Speckle as a Probe of Multi-Dimensional Entanglement, Phys. Rev. Lett. **102**, 193601 (2009).

[23] A. R. C. Buarque, W. S. Dias, F. A. B. F. de Moura, M. L. Lyra, and G. M. A. Almeida, Rogue waves in discrete-time quantum walks, Phys. Rev. A **106**, 012414 (2022).

[24] A. R. C. Buarque, W. S. Dias, G. M. A. Almeida, M. L. Lyra, and F. A. B. F. de Moura, Rogue waves in quantum lattices with correlated disorder, Phys. Rev. A **107**, 012425 (2023).

[25] W. Kirkby, Y. Yee, K. Shi, and D. H. J. O'Dell, Caustics in quantum many-body dynamics, Phys. Rev. Res. **4**, 013105 (2022).

[26] J. M. Dudley, G. Genty, A. Mussot, A. Chabchoub, and F. Dias, Rogue waves and analogies in optics and oceanography, Nat. Rev. Phys. **1**, 675 (2019).

[27] Y. Tan, X.-D. Bai, and T. Li, Super rogue waves: Collision of rogue waves in Bose-Einstein condensate, Phys. Rev. E **106**, 014208 (2022).

[28] J. Goodman, *Speckle Phenomena in Optics: Theory and Applications*, Press Monographs (SPIE, Bellingham, WA, 2020).

[29] In general, time steps Δt of any size are valid as long as the timescale of the quantum evolution is long enough so as to wash out its embedded correlations. For practical purposes, it is better to set $\Delta t \gg J^{-1}$.

[30] Generalized K distributions result from the product of two independent gamma distributions, which have the exponential distribution as a particular case.

[31] R. Höhmann, U. Kuhl, H.-J. Stöckmann, L. Kaplan, and E. J. Heller, Freak Waves in the Linear Regime: A Microwave Study, Phys. Rev. Lett. **104**, 093901 (2010).

[32] The Kluyver-Pearson formula gives the intensity distribution for a finite number of phasors of equal amplitude. If these amplitudes are random obeying some $p_A(A)$, one must evaluate the compound distribution $\int (I|A)p_A(A)dA$, where $p(I|A)$ is the conditional intensity density function depending on knowledge of A (see Sec. 3.2.4 of Ref. [28] for details).

[33] B. Morris, B. Yadin, M. Fadel, T. Zibold, P. Treutlein, and G. Adesso, Entanglement between Identical Particles Is a Useful and Consistent Resource, Phys. Rev. X **10**, 041012 (2020).

[34] H. Di Lorenzo Pires, J. Woudenberg, and M. P. van Exter, Statistical properties of two-photon speckles, Phys. Rev. A **85**, 033807 (2012).

[35] X. Cai, H. Yang, H.-L. Shi, C. Lee, N. Andrei, and X.-W. Guan, Multiparticle Quantum Walks and Fisher Information in One-Dimensional Lattices, Phys. Rev. Lett. **127**, 100406 (2021).

[36] M. K. Giri, S. Mondal, B. P. Das, and T. Mishra, Signatures of Nontrivial Pairing in the Quantum Walk of Two-Component Bosons, Phys. Rev. Lett. **129**, 050601 (2022).